Ornithology, 2026, **00**, 1–14
https://doi.org/10.1093/ornithology/ukag001
Advance access publication 14 January 2026
Research Article

Super black plumage is prevalent among *Lepidothrix* manakins

Roberta C. Canton,[1] Able Chow,[2] Andre E. Moncrieff,[1,3] Robb T. Brumfield,[1,3] Nathan P. Lord,[1] and Brant C. Faircloth[1,3,*]

[1]Department of Biological Sciences, Louisiana State University, Baton Rouge, Louisiana, USA
[2]Department of Entomology, Louisiana State University Agricultural Center, Baton Rouge, Louisiana, USA
[3]Museum of Natural Science, Louisiana State University, Baton Rouge, Louisiana, USA

Corresponding author: brant@faircloth-lab.org

Current address: Department of Biology, University of Kentucky, Lexington, Kentucky, USA

ABSTRACT

Super black plumage has been observed across the avian phylogeny, yet few studies have examined the prevalence of super black plumage at the species and subspecies levels. One group where additional super black taxa likely exist is manakins in the genus *Lepidothrix*. Previous work on these sexually dichromatic taxa showed that male *Lepidothrix velutina* (Velvety Manakins) have super black plumage, and we observed that males of several other *Lepidothrix* taxa have black plumage with a velvety appearance that is often associated with super black barbule morphologies. Here, we combine spectrophotometry with scanning electron microscopy to examine the occurrence of super black plumage throughout *Lepidothrix*. We determine how the barbules of super black taxa differ structurally from barbules of black taxa that lack super black plumage. Our results show that 5 species and 7 subspecies of *Lepidothrix* have super black plumage, that barbules of back feathers are wider and closer together in super black taxa than in black taxa, and that the super black plumage trait appears to have evolved multiple times independently in the genus. We also show that olive-green immature males of super black taxa exhibit wider barbules that are closer together than their counterparts, suggesting the development of super black plumage begins before males molt into their definitive adult plumage.

Keywords: barbule, *Lepidothrix*, manakins, plumage, super black, SEM, spectrophotometry

How to Cite
Canton, R. C., A. Chow, A. E. Moncrieff, R. T. Brumfield, N. P. Lord, and and B. C. Faircloth (2026). Super black plumage is prevalent among *Lepidothrix* manakins. *Ornithology* 143:ukag001.

LAY SUMMARY

- Super black plumage has been reported across the avian phylogeny, but few studies have examined its occurrence at the species and subspecies levels.
- We measured reflectance, barbule width, interbarbule distance, and barbule angle in *Lepidothrix* manakins to examine the prevalence and causes of super black plumage throughout the genus.
- We found that 5 species and 7 subspecies of *Lepidothrix* have developed super black plumage, that super black plumage is associated with wider barbules that are closer together, and that the development of super black feathers begins before males reach their definitive adult plumage.
- The relatively short time spans during which super black plumage has evolved suggest the genetic mechanisms affecting this trait may be relatively simple.
- We show a previously unrecognized degree of variation in the reflectance and morphology of black feathers within a single bird genus, suggesting that additional studies of the occurrence of super black barbule morphologies across the bird Tree of Life are needed.

Plumagem super negra é prevalente em piprídeos *Lepidothrix*

RESUMO

Ao longo da filogenia de aves há várias descrições de plumagem super negra, no entanto poucos estudos examinaram a prevalência dessa plumagem no nível de espécie e subespécie. Um grupo em que provavelmente há táxons com plumagem super negra ainda não descrita é o gênero *Lepidothrix*. Um estudo anterior com esses táxons mostraram que o macho de *Lepidothrix velutina* apresenta plumagem super negra, e nós observamos que outros machos de táxons de *Lepidothrix* possuem plumagem preta com aparência de veludo, como é frequentemente descrita a plumagem super negra. Neste trabalho nós combinamos dados de espectrofotometria e microscopia eletrônica de varredura para examinar a ocorrência de plumagem super negra em todo o gênero *Lepidothrix*. Nós determinamos como as bárbulas de pena super negra diferem estruturalmente das bárbulas de penas quem não tem cor super negra. Nossos resultados mostraram que cinco espécies e sete subespécies de

Submission Date: October 8, 2025. Editorial Acceptance Date: November 20, 2025

Lepidothrix tem plumagem super negra, que bárbulas são mais grossas e próximas entre si na plumagem super negra do que nas penas que não são super negra, e que a plumagem super negra parece ter evoluído múltiplas vezes independentes neste gênero. Nós também mostramos que machos juvenis imaturos com plumagem verde oliva possuem penas com bárbulas intermediárias em grossura e proximidade uma das outras quando comparada com a morfologia de penas verde oliva de fêmeas e super negra de machos adultos. Este resultado sugere que o desenvolvimento da morfologia de pena super negra começa antes que os machos atingem a plumagem de adultos.

Keywords: super negra, *Lepidothrix*, piprídeos, plumagem, bárbulas, microscopia eletrônica de varredura, espectrofotometria

INTRODUCTION

Birds play a central role in evolutionary studies of color, helping us understand the diversity of natural colors (Stoddard and Prum 2011, McCoy and Prum 2019), how colors are produced in nature (Shawkey and D'Alba 2017), how color-producing structures evolve (Prum and Torres 2003), the genetic basis of color (Funk and Taylor 2019, Price-Waldman and Stoddard 2021), and the role color plays in speciation (Hill and McGraw 2006). Bird colors are typically produced by pigments (McGraw 2006a, 2006b), by physical nanostructures that cause light scattering (Prum 2006), or by an interaction between pigments and light-scattering nanostructures.

Several recent studies (McCoy et al. 2018, McCoy and Prum 2019) showed that physical microstructures altering the direction in which light is scattered can affect the appearance of color. By studying feathers in birds of paradise (McCoy et al. 2018) and in other species across the avian phylogeny (McCoy and Prum 2019), McCoy, Prum, and colleagues discovered that different morphologies of feather barbule microstructures (Supplementary Material Figure 1) create plumage with remarkably low reflectance by increasing the number of times light is scattered back into the feather (iterative scattering) where it is absorbed by melanin pigments. This form of structurally assisted absorption produces profoundly black plumage that can appear to humans as a velvety or matte black color. These "super black" (Yang et al. 2008) plumage patches in birds are similar in reflectance to super black patches observed in other organisms like butterflies (Davis et al. 2020a), beetles (Wong and Marek 2020, Parisotto et al. 2023), ants (Lopez et al. 2024), spiders (McCoy et al. 2019), and deep-sea fishes (Davis et al. 2020b) as well as man-made materials like "dark chameleon dimers" (Huang et al. 2016) which absorb 98%–99% of incident light at any angle between 400 and 1,400 nm.

McCoy and Prum (2019) identified super black plumage patches in 32 bird species from 15 taxonomic families and determined that these super black patches had an average reflectance of 1%, a maximum reflectance <2%, and that the reflectance spectra were uniform across wavelengths from 300 to 700 nm. Black plumage in control species ($n = 22$) had an average reflectance of 4%, a range of reflectance values from 2 to 6%, and reflectance spectra with increasing slopes at wavelengths between 600 and 700 nm. Analyses of feather microstructure using images from scanning electron microscopy (SEM) suggested that super black bird plumages resulted from 5 distinct categories of feather microstructures that enhanced the absorption of light: curved arrays, dihedral straps, dense straps, sparse straps, and brushy barbs (see figure 5 in McCoy and Prum 2019). The authors also proposed the sensory bias hypothesis of super black plumage evolution that suggests super black patches evolved to emphasize adjacent, colorful patches that play a role in signaling.

One of the species McCoy and colleagues identified as having super black plumage was *Lepidothrix velutina* (Velvety Manakin), in which they observed back feathers having an average reflectance of 1.5% compared to 6.3% reflectance of back feathers collected from *L. coronata* (Blue-capped Manakin) control individuals. Morphologically, super black plumage in *L. velutina* resulted from the sparse strap barbule morphology (McCoy and Prum 2019, Supplementary Material Figure 1C), which was observed in 3 other avian families (Anatidae, Trochilidae, and Maluridae). This observation of variation in black plumage within *Lepidothrix* species was interesting, because the genus includes 9 species and 18 subspecies (Dickinson and Christidis 2014, Moncrieff et al. 2022). We observed that specimens representing some of these species and subspecies had black plumage patches with a velvety appearance, suggesting that additional *Lepidothrix* taxa have super black plumage and making us question whether plumage morphologies were similar or different among these potentially super black *Lepidothrix* species.

Beyond the appearance of velvety, black patches in males of several species, *Lepidothrix* manakins are notable for their sexual dichromatism and delayed plumage maturation. Females and immature males have olive-green plumages (Perrins 2009). It is unknown whether females and immature males of *L. velutina* (and potentially other super black *Lepidothrix* species) exhibit similar sparse strap barbule morphologies in their green feathers, or whether these morphologies only appear in males following their transition to definitive adult plumage, which occurs after 1 or 2 plumage cycles depending on the species (Johnson and Wolfe 2017, Scholer et al. 2021). A recent phylogenetic study (Moncrieff et al. 2022) also suggested multiple origins of black or green plumages within *Lepidothrix* (Figure 1), raising questions regarding how super black plumages, if they occur in multiple *Lepidothrix* taxa, evolved.

The mating systems of *Lepidothrix* manakins, best known from studies of *L. velutina* (Skutch 1969), *L. coronata* (Durães 2009, Durães et al. 2007, 2009), and *L. serena* (Prum 1985), involve the spatial clustering of male territories into leks, where males perform visual and vocal displays for females. The high energetic investment by male *Lepidothrix* in their acrobatic displays for females (Prum 1985, Durães 2009), lack of male parental care (Skutch 1969), and presence of bright plumage patches in adult males (Igic et al. 2016) are all consistent with the hypothesis that intersexual selection strongly affects *Lepidothrix* mating systems (Alfonso et al. 2021). As a result, the importance of visual signaling within this system was another key motivation for exploring the occurrence and morphological basis of super black plumage in this group.

Here, we use spectrophotometry to assess the occurrence of super black plumage throughout *Lepidothrix*, and we use SEM to examine structural differences in super black feathers at the species and subspecies taxonomic levels. We also use SEM to examine feathers of (1) olive-green adult females and olive-green immature males of taxa where adult males are super black and (2) bright green adult males of taxa that are not black to determine whether sparse strap or other super black feather morphologies are found in green birds and how these morphologies compare.

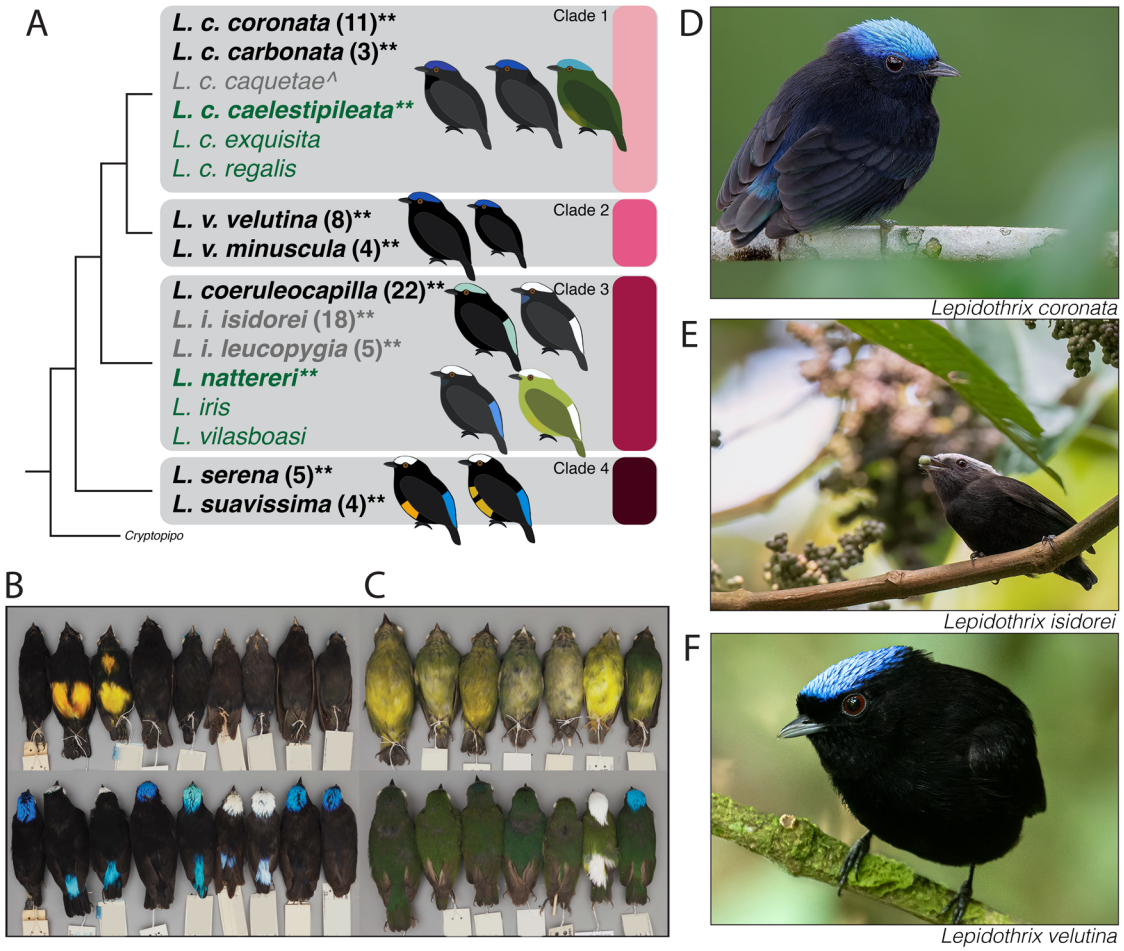

FIGURE 1. (**A**) Phylogeny of the genus *Lepidothrix* adapted from Moncrieff et al. (2022). Taxa with males having bright green plumage are listed in green font, taxa with males having black plumage are listed in gray font, taxa with males having super black plumage (determined in this study) are listed in black font. Numbers in parentheses show the count of specimens included in spectrophotometry analyses. We were unable to obtain specimens of *L. coronata caquetae*, which we have indicated with a carat. Two individuals of each taxon name in bold with asterisks were used for scanning electron microscopy. (**B**) Series of male *Lepidothrix* specimens showing the taxa in which males have black or super black plumage. Top panel shows ventral plumage and bottom panel shows dorsal plumage. Specimens (left to right): *L. velutina minuscula* LSUMZ 45456, *L. suavissima* LSUMZ 175487, *L. serena* LSUMZ 178372, *L. velutina velutina* LSUMZ 139986, *L. coeruleocapilla* LSUMZ 130304, *L. isidorei isidorei* AMNH 43008, *L. isidorei leucopygia* LSUMZ 117080, *L. coronata carbonata* LSUMZ 50981, *L. coronata coronata* LSUMZ 115767. (**C**) Series of male and female *Lepidothrix* specimens having green plumage. Top panel shows ventral plumage and bottom panel shows dorsal plumage. Specimens (left to right): *L. suavissima* (female) LSUMZ 175483, *L. coronata coronata* (female) LSUMZ 115702, *L. suavissima* (immature male) LSUMZ 175485, *L. velutina minuscula* (immature male) LSUMZ 163682, *L. coeruleocapilla* (immature male) LSUMZ 190623, *L. nattereri* (male) LSUMZ 153530, *L. coronata caelestipileata* (male) LSUMZ 133182. (**D**) Macaulay Library (ML) image of an adult male *L. coronata* taken by Matthew Bruce (ML626390794). (**E**) Image of an adult male *L. isidorei* taken by Brad Murphy (ML625067995). (**F**) Image of an adult male *L. velutina* taken by David Monroy Rengifo (ML298008331). All images used with permission of the photographers.

METHODS

Sampling Design: Spectrophotometry

There are 9 species and 18 subspecies of *Lepidothrix* (Dickinson and Christidis 2014, Moncrieff et al. 2022). Six of these species and 10 of these subspecies include adult male *Lepidothrix* that have black plumage (Figure 1). We used specimen collection databases to identify a sample of 80 male *Lepidothrix* specimens from all 6 species and 9 of the 10 subspecies where adult males appear black (Perrins 2009, Dickinson and Christidis 2014, Del Hoyo and Collar 2016, Moncrieff et al. 2022). We were unable to obtain specimens of *L. coronata caquetae*. Because black *L. coronata* are known to hybridize with green *L. coronata caelestipileata*, resulting in highly variable phenotypes across their contact zone (de Abreu et al. 2018, Moncrieff et al. 2024), we limited our selection of specimens representing *L. coronata coronata* to one locality in the Department of Loreto, Peru, since these individuals have a relatively homogeneous phenotype that we considered "typical" *L. coronata coronata*. Because our initial goal was to study the presence or absence of super black plumage among *Lepidothrix*, we did not request loans of or collect reflectance data from the 3 species where male definitive plumage is bright green (*L. nattereri*, *L. iris*, and *L. vilasboasi*).

Spectrophotometry

We measured reflectance spectra from the nape, back, throat, belly, wing, and tail plumage patches (Supplementary Material Figure 2) that appeared black in male specimens. Because our principal goal was to study variation in black color, we did not collect reflectance data from certain body patches that were not black in all species (e.g., crown and rump). Additionally, although the belly plumage patches in *L. suavissima* and *L. serena* are predominantly orange or yellow (Figure 1A and B;

Supplementary Material Figure 2), we included belly measurements for these species by targeting the black plumage on the anterior edge of the belly patches. Because they can negatively affect reflectance measurements, we did not collect data from plumage patches that were missing large numbers of feathers or with exposed skin. We also avoided plumage patches where feathers were not sitting flat on the specimen. These quality requirements led to variation among specimens in the total count of patches measured.

We collected directional reflectance data (300–700 nm) from plumage patches in a windowless, dark room using a FLAME-T-XR1-ES spectrometer along with a DH-2000-BAL deuterium-halogen lamp and a QR400-7-SR bifurcated fiber-optic probe (Ocean Optics, Inc.). Prior to each data collection session, we used the WS-1-SL diffuse reflectance standard (Ocean Optics, Inc.) as our white standard and made one measurement with all lights off to set the dark standard, and we repeated this process at 30-min intervals when data collection sessions were >30 min in length. After standardizing, we placed specimens on an adjustable platform, secured the fiber optic probe in a stand, and used the platform to raise and lower the specimen, ensuring (1) the distance between the probe and plumage patch was ~3 mm and (2) the placement of the probe was perpendicular to the plumage patch. To account for intrapatch variation in reflectance, we collected 3 measurements in an approximately triangular pattern inside the general boundaries of each plumage patch by manipulating the specimen on the stand underneath the probe. We used Ocean View (v1.6.7, Ocean Optics, Inc.) software to export raw data into text files for each measurement.

We imported the raw data into pavo v2.9.0 (Maia et al. 2019) and used the *procspec* function to smooth the reflectance spectra using LOESS smoothing with a span of 0.3 and set negative reflectance values to zero. After smoothing, we used *explorespec* to visualize the reproducibility of the 3 measurements collected from each plumage patch, and we removed a small number of measurements where individual reflectance spectra substantially differed among replicate measurements. Then, we used *aggspec* to aggregate (combine by averaging) the multiple spectral measurements collected from each plumage patch, and we used the *summary* function to compute "mean brightness" (B2), which is the mean relative reflectance over the entire spectral range (Delhey et al. 2003, Siefferman and Hill 2005). We refer to the mean brightness values as reflectance or mean reflectance. We also computed the "flatness" or slope of reflectance curves for each plumage patch between 600 and 700 nm (McCoy et al. 2018) using the mean reflectance values at each of these 2 wavelengths. We computed these values with the expectation that super black plumages would exhibit flatter slopes at 600–700 nm wavelengths relative to black plumages because structurally enhanced absorption in super black feathers produces flatter reflectance curves (Galván and Wakamatsu 2016, McCoy et al. 2018, McCoy and Prum 2019).

Although color is a continuous variable, we defined super black patches as those having mean reflectance values <2% (McCoy and Prum 2019), and we refer to all other plumage patches in other shades of black having reflectance values ≥2% as black. We imported mean reflectance values and slopes to R (R Core Team 2024), and we used R functions and *dplyr* (v1.1.2) to compute the mean and variance (±SD) of reflectance for each plumage patch by taxon. To account for the possibility that unequal sample sizes for each taxon could bias our classification of patches using mean reflectance values, we also used R and *dplyr* to generate 10 random subsamples (without replacement) of the data where sample sizes were the same for each taxon ($n = 2$). For each patch in each taxon, we computed the mean reflectance value in the subsample, counted the number of subsamples that maintained a mean reflectance <2%, and divided this count by the total number of subsamples to compute a percentage.

Following our operational definition of super black versus black patches, we called taxa super black when (1) they possessed a patch having reflectance below 2% and (2) a majority of random subsamples for that patch also had mean reflectance <2%. We called taxa black when they did not possess any super black patches. We used boxplots in *ggplot2* (Wickham 2016) to compare reflectance by plumage patch and taxon, and we used Welch's *t*-tests in *ggstatsplot* (Patil 2021) to examine the relationship between plumage patch category (super black versus black) relative to (1) mean reflectance and (2) slope of spectral profiles from 600 to 700 nm. We also used line plots in *ggplot2* to visualize overall spectral profiles (300–700 nm). Based on our assignment of black and super black patches, species, and subspecies, we identified super black versus black taxa on a phylogeny of *Lepidothrix* (Figure 1) adapted from Moncrieff et al. (2022).

We were interested in testing how many times super black plumage arose in *Lepidothrix*, so we performed ancestral state reconstruction for different plumage states using a phylogeny for the group derived from data collected by Moncrieff et al. (2022). Specifically, we pruned their linked, 75% complete dataset to include one tip per taxon, except for *L. coronata caquetae*, which we excluded because we were unable to obtain a specimen of this taxon. Then, we used IQ-TREE (v2.2.2.6, Minh et al. 2020) to infer a maximum-likelihood phylogeny from these data with the best-fitting site-rate substitution model (TVM+F+ASC+R3) originally selected by Moncrieff et al. (2022) and standard nonparametric bootstrapping (Felsenstein 1985). We created several sets of discrete character data representing the plumage colors of adult males (green, black, super black) in the tree at the taxon and patch (back, throat, and nape) levels. We were primarily interested in the evolution of super black at the species and subspecies levels, but we also wanted to ensure that the ancestral state estimates were robust to differences we observed among patches across species and subspecies. We used the *ace* function in *ape* (Paradis and Schliep 2019) to reconstruct discrete ancestral states assuming an equal rates model, and we used phytools (Revell 2024) to plot the empirical Bayesian posterior probabilities at internal nodes of the *Lepidothrix* phylogeny.

To test whether differences in reflectance measurements and the slope of spectral profiles from 600 to 700 nm were explained by our assignment of taxa to black or super black categories while accounting for the covariance structures introduced by the phylogenetic relationships between the sampled individuals and the patches we measured, we used the phylogenetic generalized linear mixed model (PGLMM) function of the *phyr* (v1.1.2) package (Ives et al. 2023) with a pruned version of the phylogeny we inferred. Specifically, we dropped measurements from wing and tail patches because these were never super black in any taxa, and we tested whether the remaining reflectance measurements or slopes appeared to be a function of taxon assignment as black or super black after including phylogeny and patch as random effects and using a Gaussian error distribution. We interpreted a significant effect ($P < 0.05$) as an indication that black

and super black taxa differed in their reflectance measurements or spectral profiles from 600 to 700 nm.

Sampling Design: Microscopy

After using a large sample of individuals to determine which taxa had super black plumage, we selected a smaller set of individuals from which to collect SEM images to investigate morphological differences of feather microstructures in black and super black plumage patches. Specifically, we focused SEM analyses on feather samples from the back plumage patch because these patches exhibited the lowest intraspecies variation in terms of reflectance (Table 1, Supplementary Material Figure 3). For each of the 9 taxa, we selected the 2 specimens with the highest and lowest average values of reflectance (excluding outliers), and we collected 2 feathers from each specimen (more detail below) to help account for variation within individuals. These reductions in sample size relative to the number of specimens from which we collected spectral data were driven by a desire to minimize the destructive sampling of feathers from research specimens as well as the cost and time required to collect high-quality SEM images.

We were also interested in examining feather microstructures in olive-green adult females of black and super black taxa, olive-green immature males of super black taxa, and bright green adult males in definitive plumage (no black feathers) of taxa that are sister to black or super black taxa (Figure 1). Our goal was to investigate whether feather microstructures associated with super black feathers from the back patch were exclusive to black or super black adult males or if these same structures appeared in these other groups. Using results from our spectral analyses (Table 1) mapped onto the *Lepidothrix* phylogeny (Figure 1), we identified the following individuals for sampling: 2 olive-green adult female *L. coronata coronata* (adult males have black back plumage; clade 1), 2 olive-green adult female *L. suavissima* (adult males have super black back plumage, clade 4), 2 olive-green immature male *L. velutina minuscula* (adult males have super black back plumage, clade 2), 2 olive-green immature male *L. coeruleocapilla* (adult males have super black back plumage, clade 3), and 2 olive-green immature male *L. suavissima* (adult males have super black back plumage, clade 4). We also identified taxa for sampling where adult males are bright green but closely related to a taxon having black or super black plumage: 2 adult male *L. coronata caelestipileata*, a subspecies closely related to *L. coronata coronata* (adult males have black back plumage, clade 1) and 2 adult male *L. nattereri*, a species nested within clade 3 that includes *L. isidorei* (adult males have black back plumage) and *L. coeruleocapilla* (adult males have super black back plumage).

After identifying individuals, we collected 2 back feathers from each specimen by plucking a single feather to the left and the right of an imaginary line that bisected the back plumage patch, and we placed each feather into its own 2 mL microtube prior to SEM. We categorized feathers into plumage patch color categories based on spectrophotometry results (black and super black) or visual assessment of their relative color and the sex of the individual from which they were collected (olive-green adult females, olive-green immature males, bright green adult males).

Scanning Electron Microscopy

We prepared feathers for SEM by placing each on a Zeiss 25.4 mm × 6 mm aluminum stub (Carl Zeiss AG) with carbon adhesive tabs and coating them with a thin layer of platinum (8 minutes at 25 mA) using an EMS 550 X Sputter Coater (Electron Microscopy Sciences, Inc). Then, we collected SEM image data using a Quanta 3D DualBeam FEG FIB-SEM (FEI, Inc.) operating at 5 kV within the LSU shared instrumentation facility (SIF). Because it was proposed that morphological features reducing reflectance were found in the feather tip (McCoy and Prum 2019), which is the most visible part of the feather, we collected SEM images of barbules at the distal tip of each feather. We were primarily interested in comparing measurements of barbule width between taxa because visual comparisons of SEM images showed that barbules of black, adult male *Lepidothrix* shared the same general shape while appearing to differ primarily in their widths (Figure 3). Because we wanted to measure barbule width, we manually tilted and rotated the samples during SEM to capture several images of each feather at different angles. After collection, we identified the best images from each of the 2 feathers for each specimen that enabled us to measure the largest number of unique barbules.

We imported selected images to ImageJ v1.54g (Schneider et al. 2012), measured the length of the scale bar in pixels, and converted that to micrometers (μm) using the *Set scale* function. Then, we used the *Straight line tool* to measure barbule width (μm). Because barbules differ in their width along their length, we wanted to account for this variation to the greatest degree possible, so we collected barbule width measurements at approximately equidistant positions starting from the intersection of the barbule with the barb. We only collected barbule measurements where the entire structure–including all margins and the intersection of the barbule with the barb–was visible. We imported measurements to R, we used the boxplot function in *ggplot2* to visualize and compare measurements among taxa, and we used a combination of Welch's *t*-tests and Welch's one-way analysis of variances (ANOVAs) in *ggstatsplot* to examine relationships between plumage patch color category and barbule width. The comparisons we conducted were: black versus super black feathers, grouped as (1) general categories and (2) by taxon; all colors grouped as general categories; and within-species comparisons of olive-green adult females, olive-green immature males, and super black males by taxon. When we used one-way ANOVAs to compare among multiple groups, we performed pairwise comparisons between subjects (Games-Howell test; Pohlert 2024) with Holm adjusted *P*-values.

In addition to barbule width, interbarbule distance and barbule angle have been associated with changes in reflectance (McCoy et al. 2019), so we collected measurements for each of these morphological features. To measure interbarbule distances, we selected SEM images for each taxon where the junction of the barbule and the barb were clearly visible. Then, to facilitate data collection, we used Procreate version 5.3.14 (Savage Interactive Pty Ltd, Hobart, Tasmania) with an Apple iPad and an Apple Pen to create a layer on top of this image where we drew straight line segments along each side of the barb and placed dots at the visible junctions of the barbules with the barb along these straight lines. We saved the modified image as a TIFF file and imported each file to ImageJ. Within ImageJ, we obtained the length of the scale bar in pixels and converted that to micrometers using the *Set scale* function, then we computed the length of the line segments between the dots that we used to indicate the junctions of barbs and barbules on each side of the feather using the *Straight line tool* (Supplementary Material Figure 4A). We imported measurements to R, we used the boxplot function in *ggplot2* to visualize and

TABLE 1. Summary of mean reflectance across 6 different plumage patches for 6 species and 9 of the 10 subspecies of *Lepidothrix* that exhibit black plumage.

Nape				Back			
Species	Mean	SD	RS	Species	Mean	SD	RS
L. serena	**1.0**	**0.41**	**100%**	***L. velutina minuscula***	**1.2**	**0.28**	**100%**
L. velutina minuscula	**1.3**	**0.55**	**100%**	***L. serena***	**1.6**	**0.24**	**100%**
L. coeruleocapilla	**1.4**	**0.37**	**100%**	***L. suavissima***	**1.6**	**0.39**	**100%**
L. suavissima	**1.4**	**0.55**	**100%**	***L. coeruleocapilla***	**1.7**	**0.48**	**80%**
L. velutina velutina	**1.5**	**0.42**	**100%**	***L. velutina velutina***	**1.8**	**0.37**	**70%**
L. coronata carbonata	**1.6**	**0.18**	**100%**	*L. isidorei isidorei*	2.1	0.62	60%
L. isidorei isidorei	2.7	0.55	0%	*L. coronata carbonata*	2.4	0.29	0%
L. coronata coronata	2.7	0.5	0%	*L. isidorei leucopygia*	2.4	0.17	0%
L. isidorei leucopygia	2.7	0.87	1%	*L. coronata coronata*	3.3	0.61	0%
Throat				**Belly**			
Species	Mean	SD	RS	Species	Mean	SD	RS
L. suavissima	**0.9**	**0.53**	**100%**	***L. suavissima***	**1.8**	**0.08**	**100%**
L. serena	**1.3**	**0.42**	**100%**	*L. velutina minuscula*	2.2	0.89	40%
L. velutina minuscula	**1.4**	**0.32**	**100%**	*L. serena*	2.4	0.55	0%
L. velutina velutina	**1.5**	**0.52**	**90%**	*L. coeruleocapilla*	2.6	0.64	20%
L. coronata coronata	**1.8**	**0.49**	**60%**	*L. velutina velutina*	2.6	1.18	30%
L. coeruleocapilla	2.1	0.47	30%	*L. coronata carbonata*	2.8	0.21	0%
L. coronata carbonata	2.6	0.09	0%	*L. isidorei isidorei*	4.0	1.07	0%
L. isidorei leucopygia	3.8	1.66	0%	*L. isidorei leucopygia*	4.4	0.61	0%
L. isidorei isidorei	4	0.94	0%	*L. coronata coronata*	4.7	0.96	0%
Wing				**Tail**			
Species	Mean	SD	RS	Species	Mean	SD	RS
L. velutina minuscula	2.3	0.07	0%	*L. suavissima*	2.7	0.52	0%
L. suavissima	2.8	0.25	0%	*L. serena*	3.3	0.46	0%
L. coronata carbonata	3.2	0.59	0%	*L. velutina minuscula*	3.4	1.00	0%
L. velutina velutina	3.4	0.83	0%	*L. coeruleocapilla*	3.7	0.89	0%
L. serena	3.8	0.93	0%	*L. velutina velutina*	4.4	1.69	0%
L. coeruleocapilla	4.5	0.82	0%	*L. coronata carbonata*	4.5	0.54	0%
L. isidorei isidorei	4.9	1.11	0%	*L. isidorei leucopygia*	4.6	0.33	0%
L. coronata coronata	5.2	0.63	0%	*L. isidorei isidorei*	4.8	0.77	0%
L. isidorei leucopygia	5.6	0.76	0%	*L. coronata coronata*	5.4	0.84	0%

We calculated means and standard deviations (SD) by averaging the mean reflectance values obtained for each individual of a given taxon. Taxa are ordered by lowest to highest mean reflectance for each plumage patch. Resampling column (RS) shows the percentage of 10 resampled data sets having mean reflectance below 2% when the number of individuals included for each taxon was the same ($n = 2$). Taxa with super black patches (mean reflectance below 2% and a majority of resampled data sets <2% reflectance) are in bold. Note that *L. isidorei isidorei* was classified as super black in most of the resampled data sets for the back plumage patch, although the mean reflectance for all individuals of this taxon was >2%.

compare measurements among taxa, and we used a combination of Welch's *t*-tests and Welch's one-way ANOVAs in *ggstatsplot* to examine relationships between plumage patch color category and interbarbule distance. The comparisons we conducted were black versus super black feathers, grouped as general categories, and all colors grouped as general categories. As before, when we used one-way ANOVAs to compare among multiple groups, we performed pairwise comparisons between subjects with Holm adjusted *P*-values.

Barbule angle is a complicated parameter to measure because there are several different measurements that can be referred to as "barbule angle" (Supplementary Material Figure 4B–D). Depending on the measurement, the angle of the barbule relative to the barb also changes along its length and depends, somewhat, on the rigidity of the barbule. For this study, we measured the angle of the barbule at its junction with the barb (Supplementary Material Figure 4B and E). To collect these measurements, we identified 1 SEM image for each taxon where this junction was clearly visible for at least 3 barbules, and we used an ImageJ macro to rotate each image so that the barb was parallel to a horizontal line. Then, we drew one straight line segment from the top of the barb to its junction with the barbule and a second segment along 10–15 µm of the upper edge of the barbule, and we used the *Angle tool* to compute the angle between these 2 segments (Supplementary Material Figure 4B). We repeated this process to collect a total of 3 angle measurements for each taxon. We imported measurements to R, we used the boxplot function in *ggplot2* to visualize and compare measurements among taxa, and we used a combination of Welch's *t*-tests and Welch's one-way ANOVAs in *ggstatsplot* to examine relationships between plumage patch color category and barbule angle. The comparisons we conducted were black versus super black feathers, grouped as general categories, and all colors grouped as general categories. We performed pairwise comparisons with Holm adjusted *p*-values.

Finally, to examine the relationship between barbule width and reflectance in black and super black taxa, we computed the mean of all barbule measurements for each specimen. Then, we compared these values to the mean reflectance of the back patch for the same specimen using Pearson's correlation coefficient after testing the input data for normality with Shapiro–Wilk tests, and we visualized the results of this

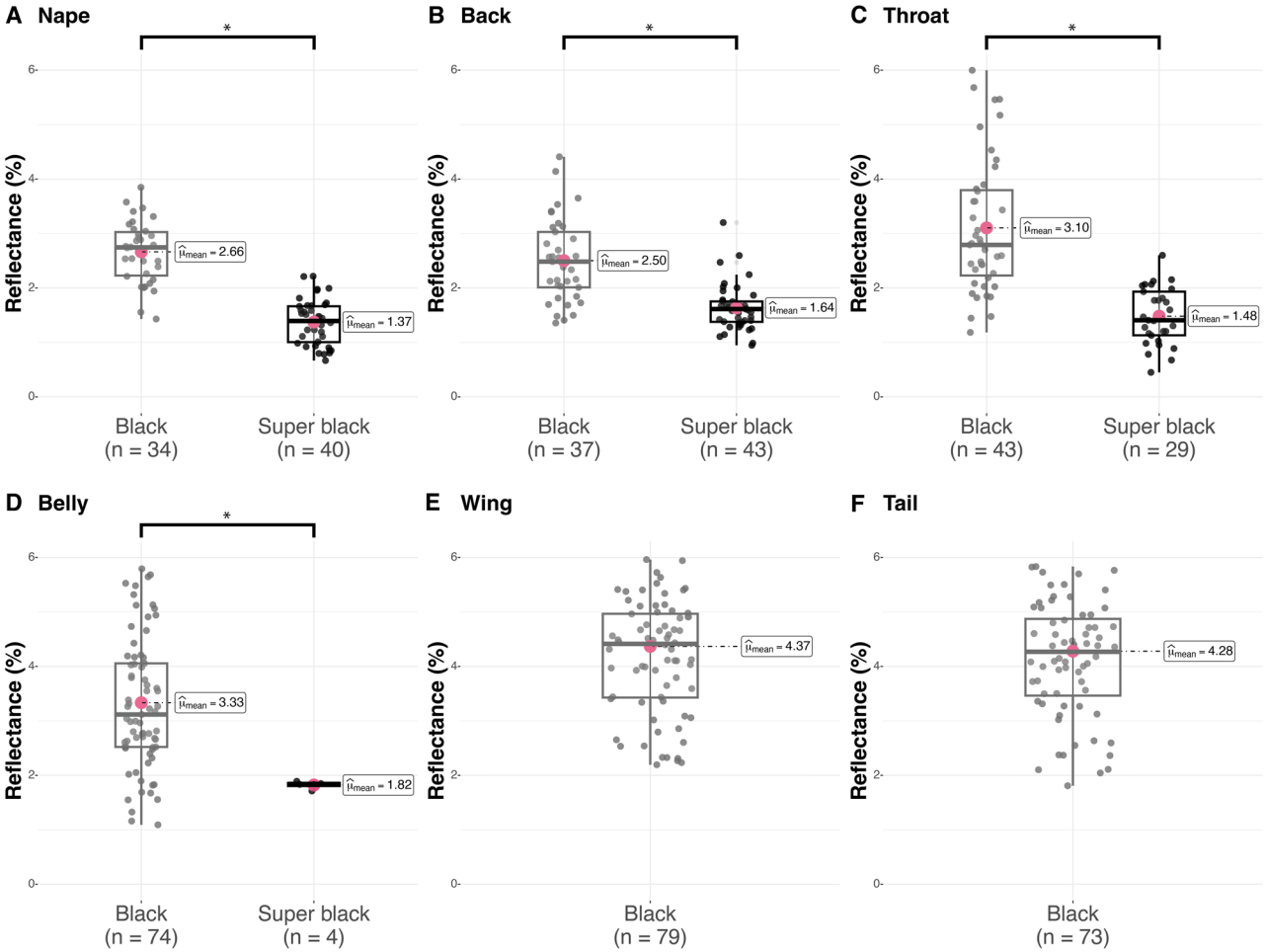

FIGURE 2. Comparison of reflectance values by plumage patch between taxa determined to have black (gray dots) and super black (black dots) plumage. Asterisks above bars indicate significantly different ($P < 0.05$) comparisons. There is no comparison for wing and tail patches because we did not observe taxa having super black wing or tail plumage patches.

test using a scatterplot produced by *ggscatterplot* from the *ggstats* package. We also used the *pglmm* function of the *phyr* package with a pruned version of the tree we inferred from the Moncrieff et al. (2022) data to perform a similar analysis that examined the relationship between reflectance, barbule width, interbarbule distance, and barbule angle using nested candidate models while accounting for the covariance structure introduced by the phylogenetic relationships between sampled individuals. We computed corrected Akaike information criterion (AIC_c) scores (Hurvich and Tsai 1989) for each model based on its number of parameters and log-likelihood values estimated by R, and we used AIC-based model comparison (Burnham & Anderson 2002) to rank and compare models.

RESULTS

Sampling and Spectrophotometry

We received loans of 62 specimens of 8 taxa from the LSU Museum of Natural Science (LSUMZ) and 18 specimens of *L. isidorei* from the American Museum of Natural History (Supplementary Material Table 1). The resulting sample for spectrophotometry comprised all 6 species and 9 of the 10 subspecies of *Lepidothrix* that exhibit black plumage and included: 11 *L. coronata*, 3 *L. coronata carbonata*, 8 *L. velutina*, 4 *L. velutina minuscula*, 18 *L. isidorei*, 5 *L. isidorei leucopygia*, 22 *L. coeruleocapilla*, 5 *L. serena*, and 4 *L. suavissima*.

We collected 1,385 reflectance measurements from all patches across all individuals (2.9 measurements per patch) that we aggregated to produce 456 reflectance measurements across all patches (Table 1, Supplementary Material Figure 3). Plumage patches having the lowest reflectance values across all specimens examined were nape (1.9% ± 0.81), back (2.0% ± 0.74), and throat (2.5% ± 1.29). Belly, tail, and wing patches generally had reflectance values >2%. Seven taxa had at least one plumage patch with average reflectance <2% in the overall and resampled data sets (*L. coeruleocapilla*, *L. coronata carbonata*, *L. coronata*, *L. serena*, *L. suavissima*, *L. velutina minuscula*, *L. velutina velutina*). Super black plumage patches (nape, back, throat, belly) exhibited statistically different ($P < 0.05$) reflectance from black plumage patches (Figure 2), and the slope of reflectance values collected from super black plumage patches in the 600–700 nm wavelengths was flatter ($P < 0.05$) than black plumage patches (Supplementary Material Figure 5). This difference was also noticeable when visually comparing the spectral profiles (300–700 nm) of super black to black plumage patches (Supplementary Material Figure 6).

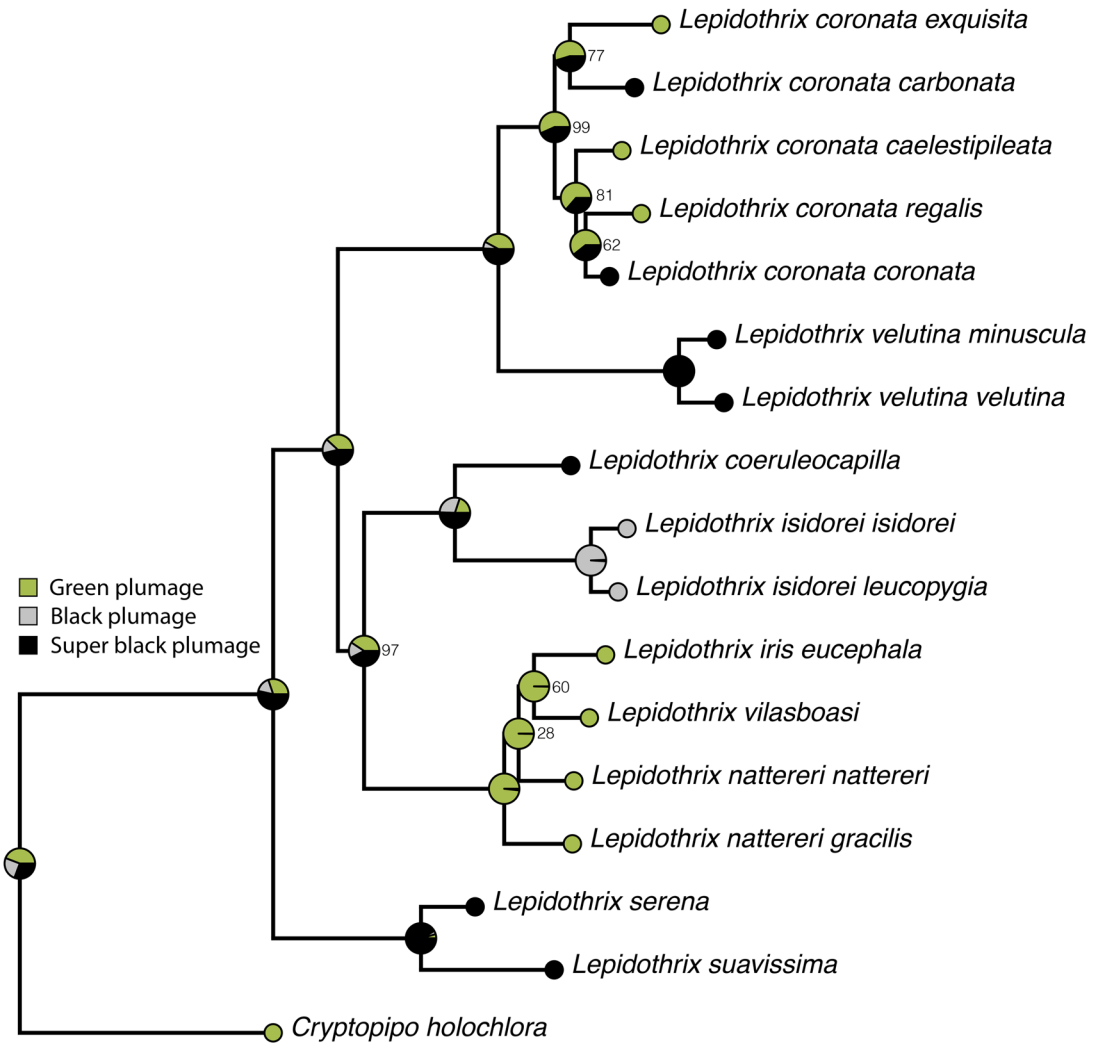

FIGURE 3. Reconstruction of ancestral plumage states for *Lepidothrix* inferred using a phylogeny derived from data collected by Moncrieff et al. (2022) and discrete character states (green, black, or super black plumage) assigned to taxa based on our spectrophotometry results (black and super black) or visual observation of specimens (green). Bootstrap support values are presented to the right of nodes when they are <100%. Results are similar when considering specific plumage patches (Supplementary Material Figure 7) versus taxa.

Wing and tail plumage patches were not super black in any *Lepidothrix* that we examined.

The pruned alignment from Moncrieff et al. (2022) included 17 tips (16 *Lepidothrix* taxa and a *Cryptopipo holochlora* outgroup) and 6,815 characters. We reduced this alignment to remove invariant sites prior to analysis, which retained 5,017 characters of which 2,374 were parsimony informative. The phylogeny we inferred (Figure 3) was similar to that resolved in the original study, except that relationships among subspecies appeared better resolved because we only included a single individual to represent each subspecies and did not collapse branches with low support to polytomies. The ancestral state reconstruction at the species and subspecies level (Figure 3) suggested that the common ancestor of all *Lepidothrix* may have had super black plumage that was inherited by *L. suavissima* and *L. serena*, that super black plumage was subsequently lost in the common ancestor to remaining *Lepidothrix*, and that the super black plumage trait evolved 4 times independently in the remaining taxa. The results when analyzing plumage patches, versus species, differed by suggesting the common ancestor of all *Lepidothrix* was likely black or green, but they were generally similar in suggesting super black plumage evolved 3 to 4 times independently within the clade (Supplementary Material Figure 7).

We also used the phylogeny to test whether differences in reflectance and spectral profiles from 600–700 nm were explained by our assignment of taxa to black or super black categories using phylogenetic generalized linear mixed models. The results of these 2 analyses showed that assignment of taxa to black or super black categories was a significant predictor ($P < 0.05$) of reflectance and spectral profiles in this range after accounting for the covariance structures introduced by the phylogenetic relationships between the sampled individuals and the patches we measured.

Scanning Electron Microscopy

We analyzed 259 SEM images collected from 64 feathers of 11 taxa and 32 specimens (Supplementary Material Tables 1 and 2) to collect 2,485 measurements of barbule width, 431 measurements of interbarbule distance, and 96 measurements of barbule angle from back feathers, including olive-green adult females of black and super black taxa, olive-green immature

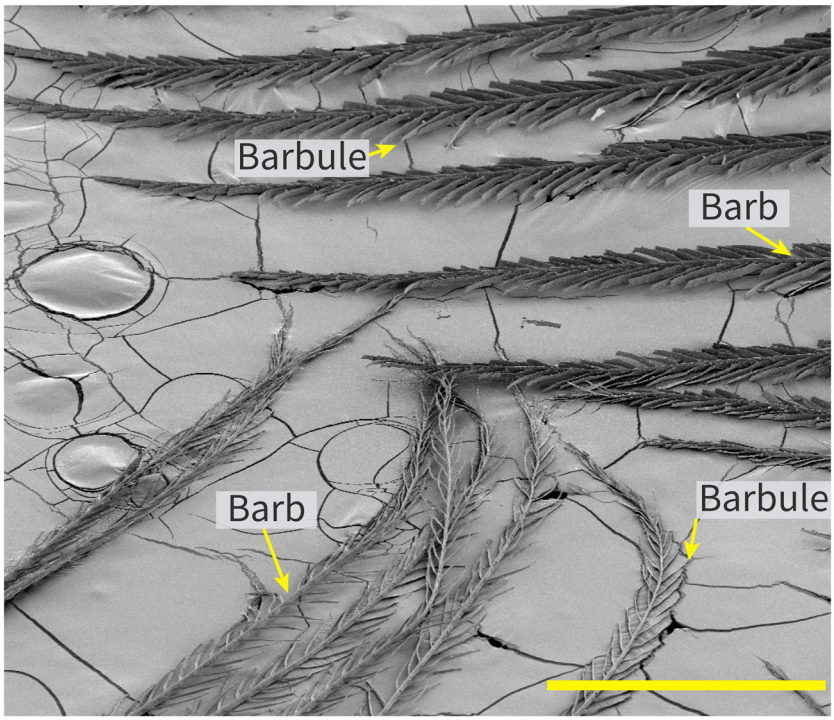

FIGURE 4. SEM image of 2 back feathers showing characteristic differences between the morphologies examined in this study: a super black *L. suavissima* feather with wider barbules at the top of the image and a black *L. coronata coronata* feather with narrower barbules at the bottom of the image. The yellow scale bar represents 500 µm.

males of super black taxa, and adult males of bright green taxa. Barbule shape of black, super black, and green feathers of males and females (Figures 4 and 5) appeared to be of the "sparse strap" type described by McCoy and Prum (2019), although we noticed that some black and super black feathers exhibited aspects of the curved array morphology (Figure 5; Supplementary Material Figure 8).

Barbule width of super black feathers was greater ($P < 0.05$) than black feathers when grouping individual taxa into black and super black plumage color categories (Supplementary Material Figure 9), as well as when comparing barbule widths of black versus super black taxa, individually (Figure 6). When we expanded the grouped comparison to include barbule widths measured from olive-green adult females, olive-green immature males, and bright green adult males, we found bright green adult males, black adult males, and olive-green adult females shared similar (albeit sometimes statistically different) barbule widths (Supplementary Material Figure 10). Olive-green immature males of super black taxa had wider barbules ($P < 0.05$) than bright green, olive-green, or black males and all females, but barbule widths of these immature individuals remained smaller than those we observed in adult males with definitive super black plumages. We observed similar results when we performed within-species analyses that compared olive-green adult females and olive-green immature males to super black adult males (Supplementary Material Figure 11–13).

Interbarbule distances of super black feathers were shorter ($P < 0.05$) than interbarbule distances of black feathers when grouping individual taxa into black and super black plumage color categories (Supplementary Material Figure 14). When we expanded the grouped comparison to include olive-green adult females, olive-green immature males of super black taxa, and bright green adult males, interbarbule distances were generally longer in bright green adult males and olive-green adult females, while those distances were reduced in black adult males, super black adult males, and olive-green immature males of super black taxa. Super black adult males and olive-green immature males of super black taxa exhibited the shortest interbarbule distances (Supplementary Material Figure 15).

Barbule angle was not different between black and super black feathers (Supplementary Material Figure 16). Similarly, the grouped comparison suggested that barbule angle is not different between most plumage color categories except for bright green adult males versus black adult males, olive-green immature males of super black taxa, and super black adult males (Supplementary Material Figure 17).

Reflectance was negatively correlated with barbule width ($r = -0.58$, $P = 0.01$; Figure 7). There was not a strong correlation between reflectance and interbarbule distance ($r = 0.30$, $P = 0.22$; Supplementary Material Figure 18) or barbule angle ($r = -0.13$, $P = 0.60$; Supplementary Material Figure 19). Barbule width remained a significant ($P < 0.05$) predictor in phylogenetic linear mixed models of reflectance that accounted for phylogeny while interbarbule distance and barbule angle were not. Comparison of nested models (Supplementary Material Table 3) explaining reflectance as a function of barbule width, interbarbule distance, or barbule angle suggested that a model of reflectance as a function of barbule width fit the data best given the candidate models analyzed, and this model was 2.9 times more likely to explain variation in reflectance than remaining models. However, one model that included barbule width and barbule angle as well as one model that included barbule width and interbarbule distance had Akaike weights that placed them within the confidence set of models (Royall 1997). A global model explaining reflectance as a function of barbule width, interbarbule distance, and barbule angle received little support.

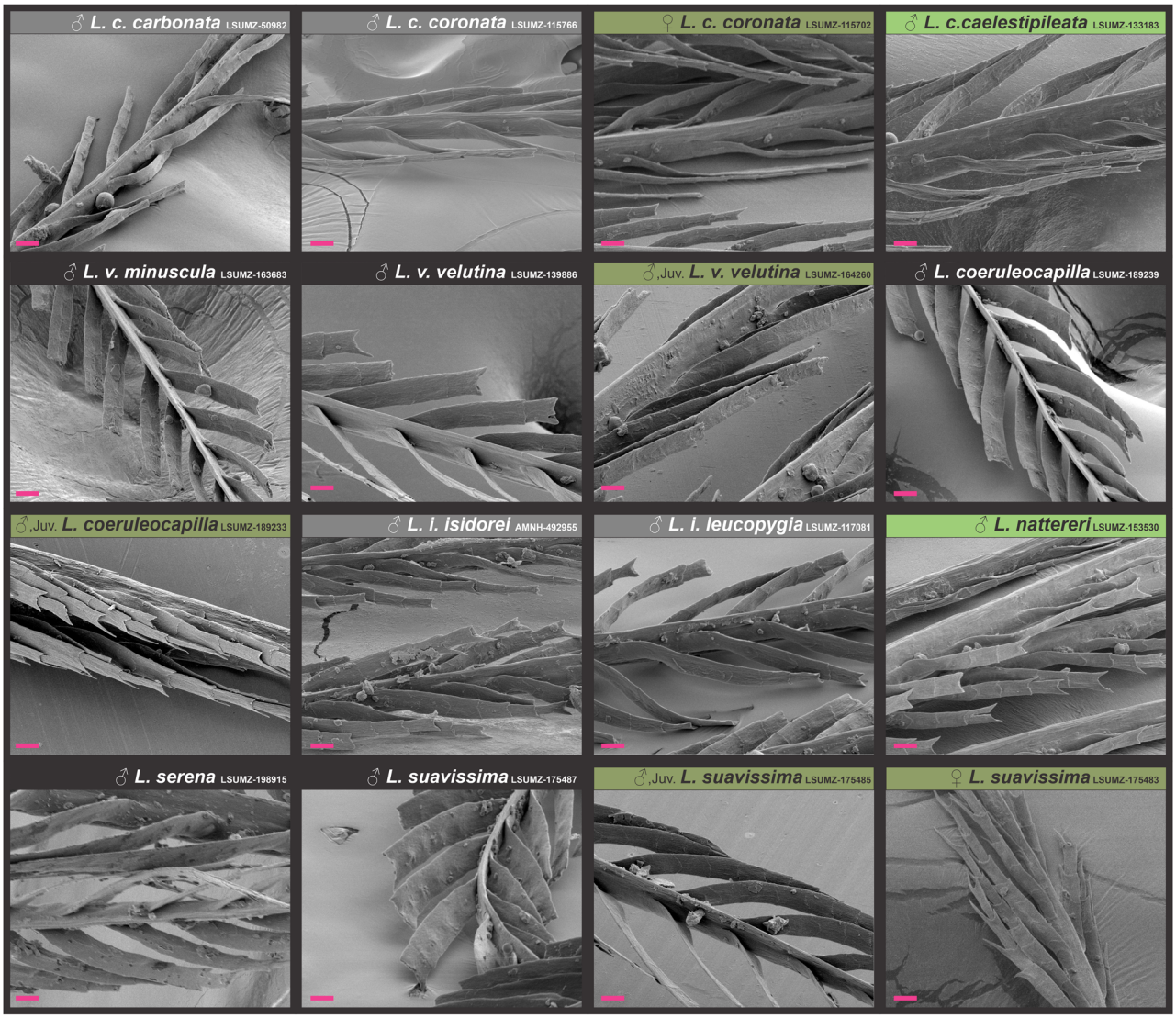

FIGURE 5. SEM images of back feathers collected from all taxa included in this study showing the differences in their barbule morphology. The header text provides the sex, taxon, and collection information for each specimen, and header backgrounds are filled according to the color of the back plumage patch: black for adult males that are super black, gray for adult males that are black, bright green for adult males that are green, and olive green for adult females and immature males that are olive green. Pink scale bars represent 10 µm.

DISCUSSION

By examining individuals of 6 *Lepidothrix* species and 9 of the 10 *Lepidothrix* subspecies where males have black plumage and using a 2% reflectance threshold to identify super black patches, we discovered that 5 *Lepidothrix* species and 7 *Lepidothrix* subspecies (Figure 1 and Table 1) have super black plumage. This includes individuals of *L. velutina*, which had previously been reported as having super black plumage (McCoy and Prum 2019) but adds 4 new species (*L. coeruleocapilla*, *L. coronata*, *L. serena*, and *L. suavissima*). In addition to having average reflectance <2%, super black patches measured among these taxa exhibited significantly reduced reflectance (Figure 2) and flatter reflectance curves (Supplementary Material Figures 5–6) than patches measured in their black relatives. Some of the reflectance values that we measured for super black patches (Table 1) illustrate that there is substantial within-taxon variation in reflectance (Supplementary Material Figure 3). For example, measurements of the back patch in *L. isidorei*, the belly patch in both *L. velutina* subspecies, and the throat patch in *L. coronata* and *L. coeruleocapilla* for some individuals fell below the 2% threshold, while other patches were above it. Variation of patch reflectance in super black taxa is also noticeable in our correlation analyses showing the relationship between mean barbule width and reflectance (Figure 7)—*L. suavissima* is a super black taxon, and the average reflectance for all *L. suavissima* individuals is below 2%, yet reflectance of the back patch in one individual (LSUMZ 68569) fell above the 2% reflectance threshold.

We also found that *L coronata* had one super black plumage patch (throat) and, given our operational definition, is a super black taxon. These observations differ from McCoy and Prum (2019), who regarded *L. coronata* as a black, control taxon in their study relative to super black *L. velutina*, although it seems their assignments were solely based on comparisons of back plumage patch reflectance where we observed similar differences between the 2 taxa. It is also difficult to notice whether *L.*

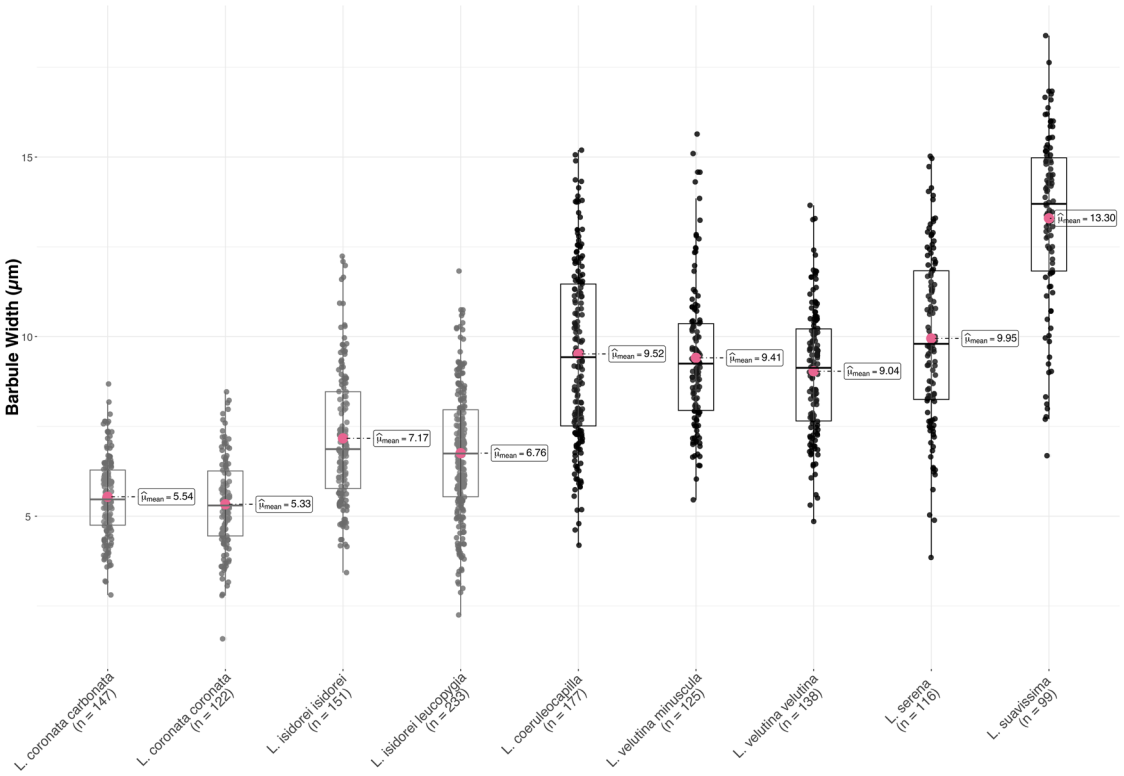

FIGURE 6. Comparison of back feather barbule width measurements between adult males of taxa classified as black (left side, gray dots and bars) and super black (right side, black dots and bars). The x-axis shows each taxon and the count of barbule widths measured for that taxon. All pairwise comparisons between barbule widths of black versus super black taxa were significantly different ($P < 0.05$) after correction for multiple tests, although we have not indicated these differences using bars and asterisks for clarity.

coronata throat plumage has a velvety appearance because this super black patch is small and surrounded by black plumage.

The Evolution of Super Black Plumage

Our results were equivocal regarding whether subspecies of super black species always possess the same super black plumage patches: both subspecies of *L. velutina* seem to follow this rule, while the 2 subspecies of *L. coronata* have different patches that are super black (throat in *L. coronata* and nape in *L. coronata carbonata*). Ancestral state reconstructions suggested that the common ancestor of all *Lepidothrix* may have been super black (Figure 3), although the reconstruction results for this node are equivocal (Figure 3 versus Supplementary Material Figure 7) and that super black plumage patches have arisen 3 to 5 times independently within the genus. The appearance of super black plumage over relatively short time frames (e.g., between closely related species like *L. coronata* and *L. velutina*) suggests that the genetic mechanisms underlying its development may be somewhat simple.

Super Black Plumage Morphology

McCoy and Prum (2019) used a phylogenetic principal component analysis (PCA) to suggest that the 2 primary features (their PC1) separating black feathers from super black feathers were (1) interbarbule distance and (2) strap-shaped barbules and that a third, secondary feature (their PC2), included barbule angle. Our results suggest that differences in barbule width (at least for back feathers) contribute more to the differences that we observed in reflectance among *Lepidothrix* taxa than differences in interbarbule distance or barbule angle (Figure 7, Supplementary Material Table 3 and Figures 18 and 19). However, we only examined a single measurement of barbule angle when there are several possible measurements (Supplementary Material Figure 4), and other measurements of barbule angle (as in Supplementary Material Figure 4D) could show stronger relationships. *Lepidothrix* barbules in all sexes of all taxa appeared to be primarily of the sparse strap morphology described by McCoy and Prum (2019). However, we noticed in several high-resolution SEM images (Figure 5, Supplementary Material Figure 8) that *Lepidothrix* barbules also sometimes exhibited morphologies with an appearance similar to curved array feathers, suggesting the possibility that combinations of microstructures sometimes enhance the absorption of light by feathers. Confusingly, we also identified black feathers that appeared to have curved array-like structures (Supplementary Material Figure 8A), so it is unclear if or how curved arrays may contribute to the increased absorption of light in *Lepidothrix*. Additional study of how different aspects of feather morphology interact to iteratively scatter light is needed.

By measuring barbule widths in olive-green adult females, bright green adult males, and olive-green immature males of super black taxa, we discovered that olive-green immature males of super black taxa have wider barbules (Supplementary Material Figure 10) than these other groups. Similarly, olive-green immature males of super black taxa have closer barbule spacing (Supplementary Material Figure 15) than most other groups, with the exception of olive-green adult females of super black taxa. These data suggest that the process of developing super black feathers begins sooner than the molt leading to the definitive male (super black) plumage but also

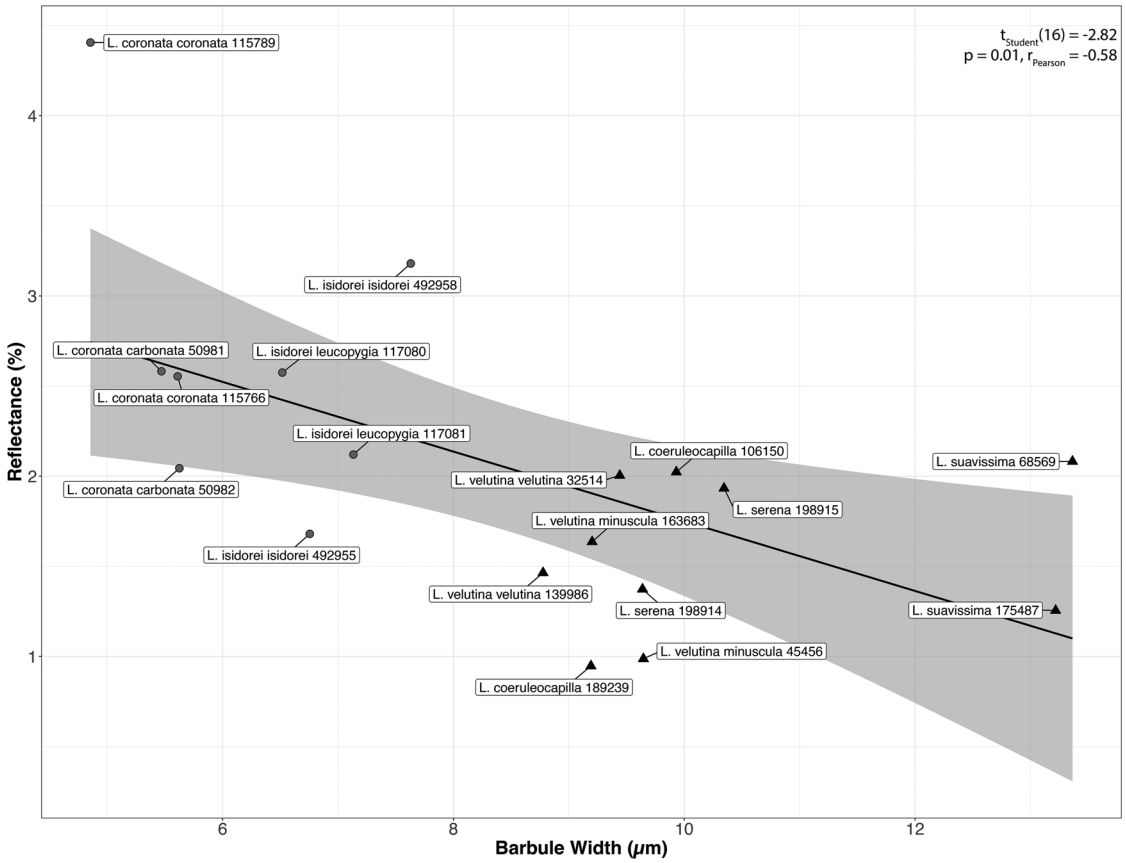

FIGURE 7. Scatterplot with a regression line showing the relationship between mean reflectance (%) and mean barbule width (μm) across taxa. Taxa with black back patches are represented by gray circles, and taxa having super black back patches are represented by black triangles. Values in the top right corner of the scatterplot show the results of Pearson's product-moment correlation test for association between barbule width and reflectance. The relationship between reflectance and barbule width remained significant ($P < 0.05$) after accounting for phylogenetic relationships between the taxa, while the relationships between reflectance and interbarbule distance (Supplementary Material Figure 18) as well as reflectance and barbule angle (Supplementary Material Figure 19) were not significant.

demonstrate that immature and adult male plumages of super black *Lepidothrix* are still quite different in terms of barbule width (and color). Taken together, these observations suggest the intriguing possibility of studying differences in expression patterns of the tissues giving rise to developing immature and adult feathers of super black taxa to help identify the loci that underlie the "switch" from olive-green to super black plumage.

The Purpose of Super Black Plumage

One hypothesis for the evolution of super black plumage patches centers around the idea of sensory bias–super black plumage (and super black patches in other organisms) evolved because it creates an optical illusion that enhances adjacent colorful patches that play a role in sexual or social signaling and selection (McCoy et al. 2018, McCoy and Prum 2019). And, in most birds, super black patches are located adjacent to colorful patches, following the predictions of this hypothesis. Most of the taxa we examined also follow these predictions: in *L. serena* and *L. suavissima* the super black throat is adjacent to a bright yellow belly and the super black back is adjacent to a brilliant azure-blue rump; in *L. velutina* the super black back and nape offset a bright blue cap; in *L. coeruleocapilla* the super black nape is adjacent to a bright blue cap and the super black back is adjacent to a deep blue rump. However, this hypothesis has not been directly tested, and it is unclear how birds perceive differences in colorful plumage patches that are adjacent to black versus super black plumage patches.

We also observed some super black patches that were not directly adjacent to any colorful patch (e.g., the throat in *L. coronata coronata*), and we observed some super black patches that were adjacent to white plumage patches (e.g., the napes of *L. suavissima* and *L. serena* relative to their white forecrowns). The purpose of super black patches like these is less clear, although super black plumage patches adjacent to white plumage were also reported by McCoy and Prum (2019) for a single taxon: *Malurus alboscapulatus* (White-shouldered Fairywren).

Conclusions

By examining 6 *Lepidothrix* species and 9 of the 10 *Lepidothrix* subspecies where males have black plumage, we showed that 5 species and 7 subspecies exhibit super black plumage. The patches that are super black vary among *Lepidothrix* taxa, and there is sometimes high variance in reflectance values of a particular plumage patch within a particular taxon. Our observation of many super black *Lepidothrix* suggests that the number of species across the avian Tree of Life having super black plumage may be significantly higher than the 32 species previously reported (McCoy and Prum 2019). By identifying additional species and subspecies that are super black and studying their

barbule morphologies using SEM and other techniques, we can gain a better understanding of how these morphologies iteratively scatter light, whether there are additional categories of feather microstructures that can be used to describe super black feathers, and how these morphologies are distributed across the avian phylogeny. Identifying and studying these species will also help us understand the genetic mechanisms that underlie these interesting plumages and whether similar or different genetic changes are responsible for the development of super black plumage in different bird species.

Supplementary material

Supplementary material is available at *Ornithology* online.

Acknowledgments

We thank Brian Smith, Paul Sweet, and Tom Trombone at the American Museum of Natural History for providing loans of *L. isidorei* specimens as well providing additional specimen metadata. We also thank Yang Mu at the LSU Shared Instrumentation Facility for his help collecting SEM data. Nicholas Mason, Steve Cardiff, and Donna Dittmann at the LSU Museum of Natural Science provided access to and loans of specimens, and Steve Cardiff helped collect feathers for SEM. Matthew Bruce, Brad Murphy, and David Monroy Rengifo kindly provided permission to use the beautiful images in Figure 1. Editor Christie Riehl, Associate Editor Christopher Clark, and 2 anonymous referees provided comments that significantly improved this manuscript.

Funding statement:

Support for this work was provided to R.C.C. by a Chapman Research Grant from the American Museum of Natural History and the Graduate Student Research Award from the Society of Systematic Biologists. Additional support was provided by NSF DEB-165562 to B.C.F. and R.T.B and the LSU College of Science to B.C.F.

Conflict of interest statement

The authors declare that they have no conflicts of interest.

Author contributions

R.C.C., B.C.F., N.P.L., A.E.M., and R.T.B conceived the research idea. R.C.C., B.C.F., and N.P.L. designed the study. R.C.C., B.C.F., and A.C. collected the data. R.C.C and B.C.F. analyzed the data and wrote the paper. All authors edited the manuscript. B.C.F. supervised the research.

Data availability

Analyses reported in this article can be reproduced using the data provided by Canton et al. (2025).

LITERATURE CITED

Alfonso, C., B. C. Jones, B. J. Vernasco, and I. T. Moore (2021). Integrative studies of sexual selection in manakins, a clade of charismatic tropical birds. *Integrative and Comparative Biology* 61:1267–1280.

Burnham, K. P, and D. R. Anderson (1998). *Model Selection and Multimodel Inference: A Practical Information-Theoretic Approach*, second edition. Springer-Verlag, New York, NY, USA.

Canton, R. C., A. Chow, A. E. Moncrieff, R. T. Brumfield, N. P. Lord, and B. C. Faircloth (2025). Data from: Super black plumage is prevalent among *Lepidothrix* manakins. *Ornithology* 143:ukag001. https://doi.org/10.6084/m9.figshare.28582217 [Dataset].

de Abreu, F. H. T., J. Schietti, and M. Anciães (2018). Spatial and environmental correlates of intraspecific morphological variation in three species of passerine birds from the Purus–Madeira interfluvium, Central Amazonia. *Evolutionary Ecology* 32:191–214.

Davis, A. L., H. F. Nijhout, and S. Johnsen (2020a). Diverse nanostructures underlie thin ultra-black scales in butterflies. *Nature Communications* 11:1294.

Davis, A. L., K. N. Thomas, F. E. Goetz, B. H. Robison, S. Johnsen, and K. J. Osborn (2020b). Ultra-black camouflage in deep-sea fishes. *Current Biology: CB* 30:3470–3476.e3.

Delhey, K., A. Johnsen, A. Peters, S. Andersson, and B. Kempenaers (2003). Paternity analysis reveals opposing selection pressures on crown coloration in the Blue Tit (*Parus caeruleus*). *Proceedings. Biological Sciences* 270:2057–2063.

Del Hoyo, J., and N. J. Collar (2016). *HBW and BirdLife International Illustrated Checklist of the Birds of the World*. Lynx Edicions, Barcelona, Spain.

Dickinson E. C, and L. Christidis (Editors) (2014). *The Howard & Moore Complete Checklist of the Birds of the World*, 4th edition. Aves Press, Eastbourne, UK.

Durães, R. (2009). Lek structure and male display repertoire of blue-crowned manakins in Eastern Ecuador. *The Condor* 111:453–461.

Durães, R., B. A. Loiselle, and J. G. Blake (2007). Intersexual spatial relationships in a lekking species: Blue-crowned Manakins and female hot spots. *Behavioral Ecology* 18:1029–1039.

Durães, R., B. A. Loiselle, P. G. Parker, and J. G. Blake (2009). Female mate choice across spatial scales: Influence of lek and male attributes on mating success of blue-crowned manakins. *Proceedings. Biological Sciences* 276:1875–1881.

Felsenstein, J. (1985). Confidence limits on phylogenies: An approach using the bootstrap. *Evolution; International Journal of Organic Evolution* 39:783–791.

Funk, E. R., and S. A. Taylor (2019). High-throughput sequencing is revealing genetic associations with avian plumage color. *The Auk* 136:1–7.

Galván, I, and K. Wakamatsu (2016). Color measurement of the animal integument predicts the content of specific melanin forms. *RSC Advances* 6:79135–79142.

Hill, G. E, and K. J. McGraw (Editors) (2006). *Bird Coloration*. Harvard University Press, Cambridge, MA, USA.

Huang, J., C. Liu, Y. Zhu, S. Masala, E. Alarousu, Y. Han, and A. Fratalocchi (2016). Harnessing structural darkness in the visible and infrared wavelengths for a new source of light. *Nature Nanotechnology* 11:60–66.

Hurvich, C. M., and C. L. Tsai (1989). Regression and time series model selection in small samples. *Biometrika* 76:297–307.

Igic, B., L. D'Alba, and M. D. Shawkey (2016). Manakins can produce iridescent and bright feather colours without melanosomes. *The Journal of Experimental Biology* 219:1851–1859.

Ives, A. R. Dinnage, L. A. Nell, M. Helmus, and D. Li (2023). phyr: Model based phylogenetic analysis. https://daijiang.github.io/phyr/

Johnson, E. I, and J. D. Wolfe (2017). *Molt in Neotropical Birds: Life History and Aging Criteria*. CRC Press, Boca Raton, FL, USA.

Lopez, V. M., W. Krings, J. R. Machado, S. Gorb, and R. Guillermo-Ferreira (2024). Ultrablack color in velvet ant cuticle. *Beilstein Journal of Nanotechnology* 15:1554–1565.

Maia, R., H. Gruson, J. A. Endler, and T. E. White (2019). Pavo 2: New tools for the spectral and spatial analysis of colour in r. *Methods in Ecology and Evolution* 10:1097–1107.

McCoy, D. E., A. J. Shultz, C. Vidoudez, E. van der Heide, J. E. Dall, S. A. Trauger, and D. Haig (2021). Microstructures amplify carotenoid plumage signals in tanagers. *Scientific Reports* 11:8582.

McCoy, D. E., T. Feo, T. A. Harvey, and R. O. Prum (2018). Structural absorption by barbule microstructures of super black bird of paradise feathers. *Nature Communications* 9:1.

McCoy, D. E., V. E. McCoy, N. K. Mandsberg, A. V. Shneidman, J. Aizenberg, R. O. Prum, and D. Haig (2019). Structurally assisted super black in colourful peacock spiders. *Proceedings. Biological Sciences* 286:20190589.

McCoy, D. E., and R. O. Prum (2019). Convergent evolution of super black plumage near bright color in 15 bird families. *Journal of Experimental Biology* 222:1–13.

McGraw, K. J. (2006a). Mechanics of melanin-based coloration. In *Bird Coloration* (G. E. Hill and K. J. McGraw, Editors). Harvard University Press, Cambridge, MA, USA. pp. 243–294.

McGraw, K. J. (2006b). Mechanics of carotenoid-based coloration. In *Bird Coloration* (G. E. Hill and K. J. McGraw, Editors). Harvard University Press, Cambridge, MA, USA. pp. 177–242.

Minh, B. Q., H. A. Schmidt, O. Chernomor, D. Schrempf, M. D. Woodhams, A. von Haeseler, and R. Lanfear (2020). IQ-TREE 2: New models and efficient methods for phylogenetic inference in the genomic era. *Molecular Biology and Evolution* 37:1530–1534.

Moncrieff, A. E., B. C. Faircloth, and R. T. Brumfield (2022). Systematics of *Lepidothrix manakins* (Aves: Passeriformes: Pipridae) using RADcap markers. *Molecular Phylogenetics and Evolution* 173: 107525–107513.

Moncrieff, A. E., B. C. Faircloth, R. C. Remsen, A. E. Hiller, C. Felix, A. P. Capparella, A. Aleixo, T. Valqui, and R. T. Brumfield (2024). Implications of headwater contact zones for the riverine barrier hypothesis: A case study of the blue-capped manakin (*Lepidothrix coronata*). *Evolution; International Journal of Organic Evolution* 78:53–68.

Paradis, E, and K. Schliep (2019). Ape 5.0: an environment for modern phylogenetics and evolutionary analyses in R. *Bioinformatics (Oxford, England)* 35:526–528.

Parisotto, A., V. V. Vogler-Neuling, U. Steiner, M. Saba, and B. D. Wilts (2023). Structural light absorption in elytral micropillars of *Euprotaetia inexpectata* beetles. *Materials Today Advances* 19:100399.

Patil, I. (2021). Visualizations with statistical details: the "ggstatsplot" approach. *Journal of Open Source Software* 6:3167.

C., Perrins (Editor) (2009). *The Princeton Encyclopedia of Birds*. Princeton University Press, Princeton, NJ, USA.

Pohlert, T. (2024). Calculate pairwise multiple comparisons of mean rank sums extended. https://CRAN.R-project.org/package=PMCMRplus

Price-Waldman, R, and M. C. Stoddard (2021). Avian coloration genetics: Recent advances and emerging questions. *The Journal of Heredity* 112:395–416.

Prum, R. O. (1985). Observations of the White-fronted Manakin (*Pipra serena*) in Suriname. *The Auk* 102:384–387.

Prum, R. O. (2006). Anatomy, physics, and evolution of structural colors. In *Bird Coloration* (G. E. Hill and K. J. McGraw, Editors). Harvard University Press, Cambridge, MA, USA, pp. 295–353.

Prum, R. O., and R. Torres (2003). Structural colouration of avian skin: Convergent evolution of coherently scattering dermal collagen arrays. *The Journal of Experimental Biology* 206:2409–2429.

R Core Team (2024). R: A language and environment for statistical computing. *R Foundation for Statistical Computing*. Vienna, Austria. https://www.R-project.org

Revell, L. J. (2024). Phytools 2.0: An updated R ecosystem for phylogenetic comparative methods (and other things). *PeerJ* 12:e16505.

Royall, R. M. (1997). *Statistical Evidence: A Likelihood Paradigm*. Chapman and Hall, New York, NY, USA.

Schneider, C. A., W. S. Rasband, and K. W. Eliceiri (2012). NIH image to ImageJ: 25 years of image analysis. *Nature Methods* 9:671–675.

Scholer, M. N., J. C. Kennedy, B. H. Carnes, and J. E. Jankowski (2021). Preformative molt, plumage maturation, and age criteria for 7 species of manakins. *The Wilson Journal of Ornithology* 133:379–526.

Shawkey, M. D., and L. D'Alba (2017). Interactions between colour-producing mechanisms and their effects on the integumentary colour palette. *Philosophical Transactions of the Royal Society of London. Series B, Biological Sciences* 372:20160536.

Siefferman, L., and G. E. Hill (2005). UV-blue structural coloration and competition for nestboxes in male Eastern bluebirds. *Animal Behaviour* 69:67–72.

Skutch, A. F. (1969). Life histories of Central American birds: Families cotingidae, pipridae, formicariidae, furnariidae, dendrocolaptidae, and picidae. *III. Pacific Coast Avifauna* 35:1–580.

Stoddard, M. C., and R. O. Prum (2011). How colorful are birds? Evolution of the avian plumage color gamut. *Behavioral Ecology* 22:1042–1052.

Wickham, H. (2016). *ggplot2: Elegant Graphics for Data Analysis*. Springer-Verlag New York, NY, USA.

Wong, V. L., and P. E. Marek (2020). Structure and pigment make the eyed elater's eyespots black. *PeerJ* 8:e8161.

Yang, Z.-P., L. Ci, J. A. Bur, S.-Y. Lin, and P. M. Ajayan (2008). Experimental observation of an extremely dark material made by a low-density nanotube array. *Nano Letters* 8:446–451.